Supporting information

S1. Experimental details.

To synthesis of new phase hollandite-type VOOH: 1 mmol $V(OH)_2NH_2$ precursor [1], 1 mmol NH_4F, was mixed together with 0.400 mL 1-butyl-3-methylimidazolium tetrafluoroborate $[BMIM][BF_4]$ ionic liquid (2 M) aqueous solution in a 4 mL microwave vial kit. After the mixture had been stirred for 2 min to form a transparent solution, the microwave vial kit was sealed and placed into microwave heating equipment (Biotage, Model: Initiator EXP EU 355301), and then heated at 160 °C for 6 h. The system was then allowed to cool to room temperature. The final black hollandite-type VOOH product was collected by centrifugation, and washed with deionized water and ethanol to remove any possible ionic remnants, then dried in vacuum at 50 ^{o}C.

Characterization**:** The sample was characterized using XRD with a Philips X'Pert Pro Super diffractometer with Cu Kα radiation (λ = 1.54178 Å). XPS measurements were performed on a VGESCALAB MKII X-ray photoelectron spectrometer with an excitation source of Mg Ka = 1253.6 eV. The field emission scanning electron microscopy (FE-SEM) images were taken on a JEOL JSM-6700F scanning electron microscope. The TEM images were obtained on a JEOL-2010 transmission electron microscope at an acceleration voltage of 200 kV. The electrical resistivity of the as-prepared hollandite-type VOOH was measured with the use of a computer-controlled, four-probe technique. Electrical contacts consisted of fine gold wire attached to the crystals with silver paste. Samples were placed under vacuum for at least 24 h to allow the silver paste to dry completely, which improved contact performance. Measurements of the sample cross-sectional area and voltage probe separation were made with a calibrated binocular microscope. The magnetization was characterized by a superconducting quantum interference device (SQUID, quantum design MPMS XL-7) magnetometer in 4 and 300 K.

S2. The 2×2×6 supercell structure of new phase hollandite-type VOOH with 2×2 infinite tunnel structure

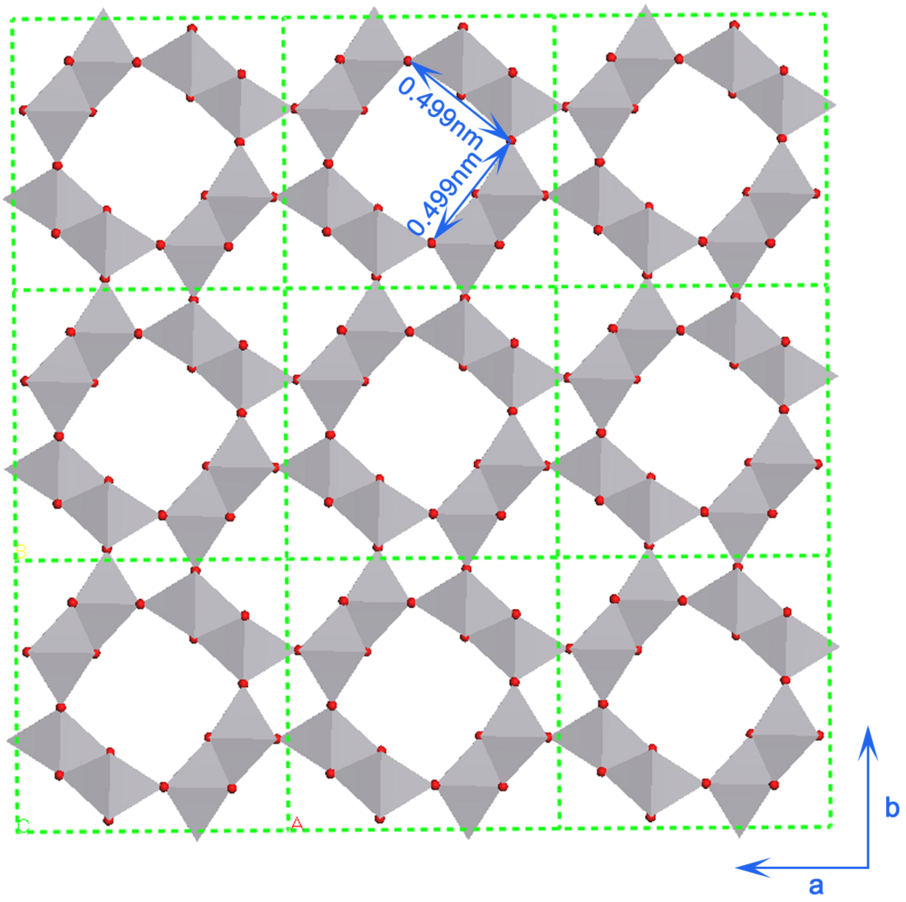

Figure S2. The 2×2×6 supercell structure of new phase hollandite-type VOOH projected along c axis.

S3. XPS spectra of new phase hollandite-type VOOH sample

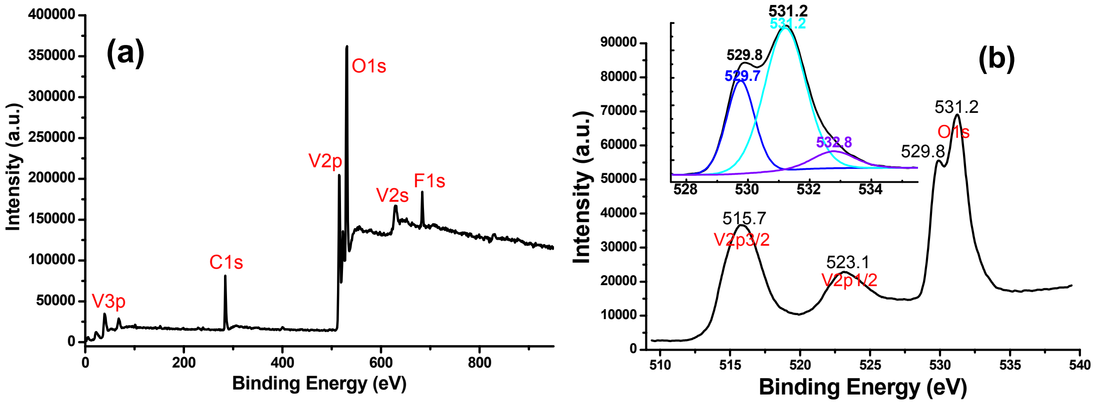

Figure S3. (a) The survey XPS spectrum of hollandite-type VOOH product, where the elements of V, O could be revealed in the spectrum and the carbon peak at 284.6 eV was taken as the reference. Notably, the hydrogen atoms were invisible in the XPS spectrum. (b) High-resolution

XPS spectrum of new phase hollandite-type VOOH hollow dandelions. Top inset in (b): fitting curves for HRXPS spectrum of O 1s region.

X-ray photoelectron spectroscopy (XPS) provides the direct information for the composition of the product as well as the valence state of vanadium ions by careful analysis of the surface molecular and electronic structure. The binding energies in the XPS spectra were corrected by referencing the C 1s 284.60 eV. Observed from the survey XPS spectra, the as-obtained sample mainly consisted of the elements of vanadium and oxygen **(Figure S3a)**, revealing it is a kind of vanadium oxide. High resolution XPS (HRXPS) for O_{1s} region (inset in **Figure S3b**) shows an asymmetry in the right part, indicating there are more than one oxygen contribution existed here: the core level centered at 529.7 eV, 531.2 eV, and 532.8 eV could be assigned to the O^{2-} in the V-O, O-H and the small amounts of physically absorbed H_2O, respectively [2], revealing that the oxygen atoms have two kinds of chemical environments of V-O bond as well as the O-H bond. Also, the V_{2p} core level spectrum (**Figure S3b**) reveals that the observed value (515.7 eV) of the binding energies for $V_{2p3/2}$ is in agreement with the literature values of V^{3+} samples [3]. In addition, the determination of the valence state of the vanadium oxides can also rely on the difference in binding energy (Δ) between the O1s and $V2p_{3/2}$ level. [4] For our product, the corresponding Δ value is found to be 14.1 eV, approaching the reported value in the literature for V^{3+} [5].

Notably, as revealed in the survey XPS spectrum in **Figure S3a**, the presence of fluorine ion (F^-) is an stabilizing anions to maintain the 2×2 tunnelled structure of hollandite VOOH. Notably, the ion stabilizing effect is similar to that in hollandite FeOOH structure. [6]

S4. Determination of vanadium oxidation state from Redox titration experiments

The vanadium oxidation state was determined by redox titration according to the following procedure: First, in the Ar-gas atmosphere, a definite amount of hollandite-type VOOH sample was dissolved quickly in a 60 ml of 1.7M H_2SO_4 solution, named **solution-(a)**. The standard $KMnO_4$ solution, which was referenced by titrating with $Na_2C_2O_4$, was employed to titrate **solution-(a)**, where the oxidation states of vanadium in the hollandite-type VOOH sample were oxidized into V(VI) in VO_2^+ ions. With the extra-addition of $KMnO_4$, the color of **solution-(a)** became yellow gradually. The sudden color change from light yellow to deep orange indicated the titration endpoint in our process. Based on the careful calculation and analysis of the titration results, the oxidation state of vanadium was reasonably calculated to be + 2.93, very approaching to +3 in our case.

S5. XRD analysis

In our case, the crystallographic lattice constant (a=10.3993 Å; c=3.0281 Å) is obtained according to the calculation of d value from the as obtained hollandite-type VOOH and the borrowed corresponding miller indices in the XRD pattern of β-FeOOH crystallographic plane (in JCPDS card No. 75-1594). Also, we perform the following equation to confirm that the all the peaks in our hollandite VOOH XRD pattern were well indexed into tetragonal with the crystallographic lattice constant of a=10.3993 Å and c=3.0281 Å.

$$d = \frac{\mathrm{a}}{\sqrt{h^2 + k^2 + l^2/(c/a)^2}}$$

The results were all summarized as followed **Table S4**, where the experimental d (Å) value agrees well with the theoretical d (Å) value, confirming that the XRD pattern obtained here can be readily indexed to the tetragonal system with the crystallographic lattice constant of a=10.3993 Å, and c=3.0281 Å. Based on the high resemblance with β -FeOOH, the formula for our vanadium oxide is hollandite VOOH from the XRD point of view. Moreover, it can be found that the calculated XRD pattern from hallandite-type VOOH cell is well agreed with the experimental pattern as shown in **Figure S5**. Therefore, our XRD results verified that our as-obtained product is new phase hollandite-type VOOH.

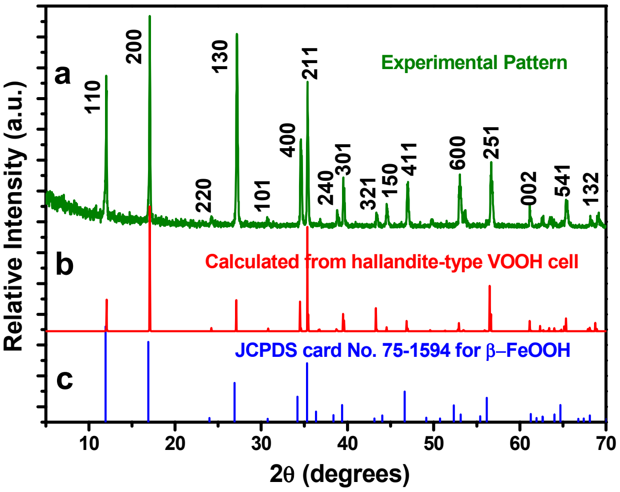

Figure S5. (a) The experimental XRD pattern of hollandite-type VOOH. (b) The calculated XRD pattern from the hollandite-type VOOH cell. (c) The standard tetragonal β -FeOOH pattern in JCPDS card NO. 75-1594.

Table S5. The summary information of the experimental d (Å) values, and the theoretical d (Å) values calculated according to the indices of crystallographic plane for β-FeOOH (JCPDS card No. 75-1594) for the as-obtained new phase VOOH.

(hkl)	Theoretical d value (Å)	Experimental d value (Å)
110	7.3534	7.3595
200	5.1997	5.1997
220	3.6767	3.6723
130	3.2886	3.2835
101	2.9076	2.9105
400	2.5998	2.5952
211	2.5378	2.5394
330	2.4511	2.4418
240	2.3254	2.3190
301	2.2806	2.2789
321	2.0886	2.0861
150	2.0395	2.0334
411	1.9381	1.9363
600	1.7332	1.7283
501	1.7144	1.7096
251	1.6282	1.6246
002	1.5141	1.5141
112	1.4830	1.4834
202	1.4537	1.4651
541	1.4312	1.4280
132	1.3753	1.3738

S6. FE-SEM images of the as-obtained quadrangular nanorods for new phase hollandite-type VOOH.

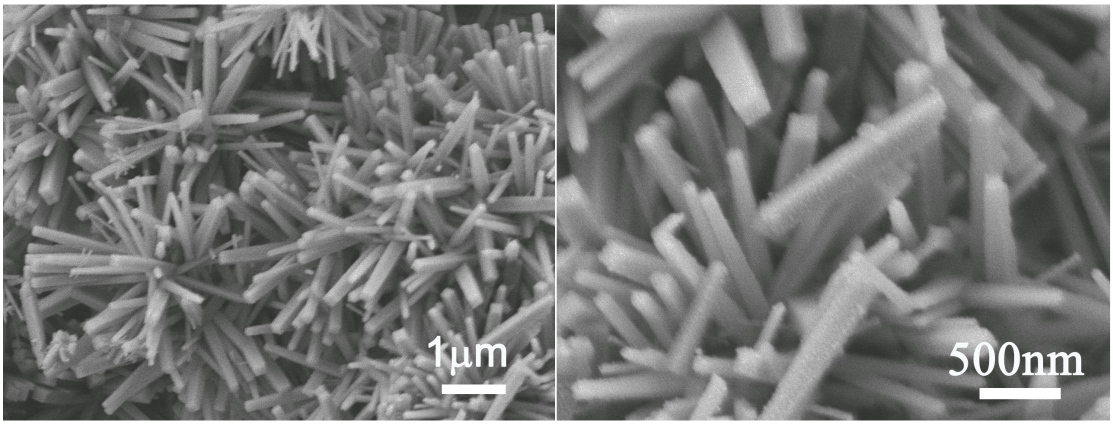

Figure S6. FE-SEM images of the as-obtained quadrangular nanorods for new phase hollandite-type VOOH, where the representative FE-SEM images of hollandite-type VOOH shows the quadrangular nanorod outlook with side width ranging from 40 nm to 300 nm and lengths up to hundreds of micrometers, revealing the large ratio of surface area of as-obtained nanorods.

S7. SAED pattern analysis

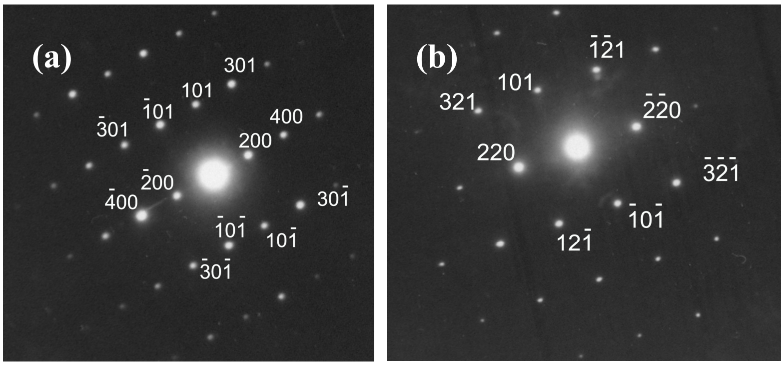

Figure S7. (a) and (b) were the SAED patterns in the inset of Figure 3a and 3c in the manuscript, respectively.

The angle values between the lattice planes that appeared in the SAED patterns provide the further evidence for new phase hollandite VOOH. The experimental angle value was achieved by directly determining the corresponding angle between the two lines, where the lines were formed by the linkage of each of two points (representing the concerned two lattice planes) with the zone-axis point in the same SAED pattern, respectively. The theoretical angle value was obtained by the crystallographic parameters calculation based on the tetragonal hollandite VOOH. The relevant formula was shown as follows:

$$Lattice\ Plane\ Angle = \frac{\frac{h_1 \times h_2 + k1 \times k2}{a \times a} + \frac{l_1 \times l_2}{c \times c}}{\sqrt{\left(\left(\frac{h_1 \times h_1 + k1 \times k1}{a \times a} + \frac{l_1 \times l_1}{c \times c}\right) \times \left(\frac{h_2 \times h_2 + k2 \times k2}{a \times a} + \frac{l_2 \times l_2}{c \times c}\right)\right)}}$$

All the experimental and calculated results were summarized in **Table S6**, where the experimental angle values agree well with the corresponding calculation ones, giving the solid evidence that the as-obtained vanadium dioxides was tetragonal hollandite VOOH.

Table S7. The summary information of the experimental angle values and the theoretical angle values for the as-obtained new phase hollandite VOOH.

Lattice Plane		Theoretical Angle Value	Experimental Angle Value
(101)	(002)	16.24	16.4
	(301)	24.91	24.8
	(501)	39.29	39.7
	(200)	73.76	73.6
	(220)	78.59	77.6
	(321)	33.84	34.6
(002)	(301)	41.16	41.0
(002)	(200)	90.00	90.0
(200)	(301)	48.84	48.7
(200)	(501)	34.47	34.5
(220)	(321)	44.75	43.2

S8. Formation mechanism of the quadrangular outlook for new phase hollandite-type VOOH

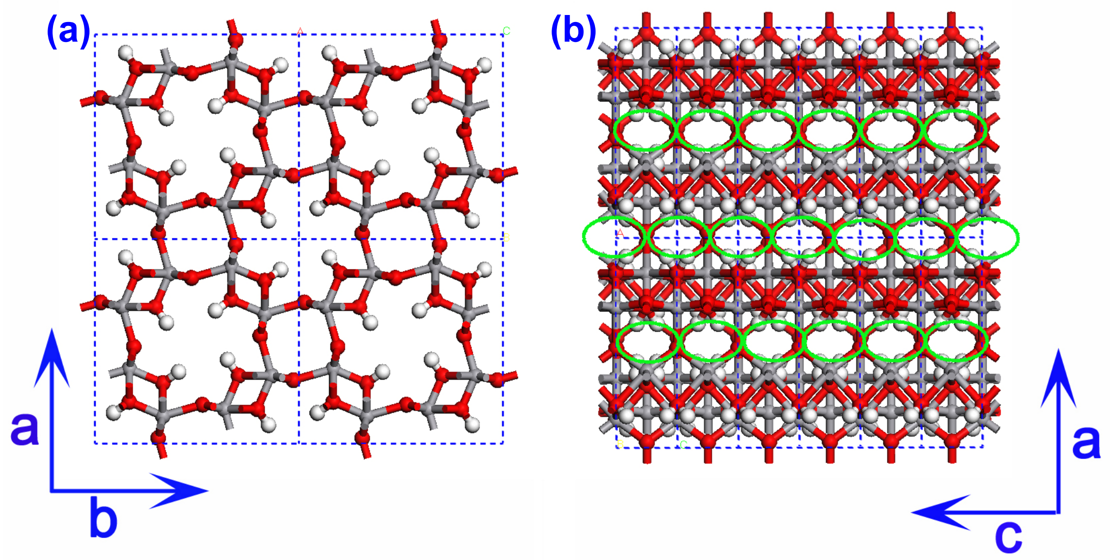

Figure S8. The 2×2×6 supercell structure of new phase hollandite-type VOOH projected along c axis (a) and b axis (b).

The appearance of quadrangular nanorod outlook for new phase hollandite-type VOOH is strongly related with the way its crystal packed. In hollandite-type VOOH, the double chains of edge-linked V^{3+}-(O, OH) octahedra shared corners to form a framework containing large 2×2 tunnels with square-cross sections that were measured to be two octahedra per side as shown in **Figure S8a**. Also, the hollandite-type VOOH has a tetragonal system with the space group of I4/m. The space group of I4/m enables the equivalence for the atomic crystal lattice between a-axis and b-axis in the hollandite-type VOOH structure. **Figure S8a** shows the 2×2×6 supercell structure of hollandite-type VOOH projected along c-axis, from which one can see that the atomic configuration were actually equivalent between a-axis and b-axis. The structural equivalent for a-axis and b-axis makes [200] and [020] the same growth rate, resulting in the formation of square outlook in a-b plane for a quadrangular cross-section of the VOOH nanorod. However, hollandite-type VOOH exhibits the staking-density difference between a-axis/b-axis and c-axis. In this case, the pore structures that appear with a separation distance of c/2 enables the larger staking density along c-axis when compared with that along a-axis/b-axis as shown in **Figure S8b**. The larger staking density along c-axis compared with a-axis/b-axis (a-axis is equivalent to b-axis for I4/m space group) resulted in the faster stacking rate along c-axis direction to form quadrangular nanorod with high length-diameter ratio along the direction of c-axis. In other words, the growth of quadrangular VOOH nanorods is actually the outward embodiment of the internal crystal structure of new phase hollandite-type VOOH.

S9. The UV-vis analysis of the hollandite-type VOOH product.

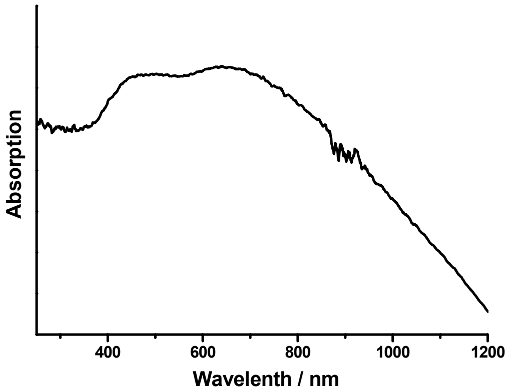

Figure S9. UV-Vis absorption spectrum of new phase hollandite-type VOOH, which was calculated from the reflection data that measured by UV-Vis reflectance spectroscopy using the solid samples. Observed from the absorption spectrum, there existed a broad absorption in the range of 400 ~ 900 nm that covers nearly whole region of visible light, giving the direct reason why the as-obtained hollandite-type VOOH sample is in the black color.

References in the supporting information

---

[1] C.Z. Wu, X.D. Zhang, B. Ning, J.L. Yang, Y. Xie, *Inorg. Chem.* 2009, **48**, 6044

[2] G. Silversmit, D. Depla, H. Poelman, G. B. Marin, R. D. Gryse, *J. Electron. Spectrosc. Relat. Phenom.* 2004, **135**, 167.

[3] (a) G.A. Sawatzki, D. Post *Phys. Rev. B.* 1979, **20**, 1546. (b) C.Z. Wu, Z.P. Hu, W. Wang, M. Zhang, J.L. Yang, Y. Xie, *Chem. Commun.* 2008, 3891.

[4] J. Mendialdua, R. Casanova, Y. Barbaux *J. Electron. Spectrosc. Relat. Phenom.* 1995, **71**, 249

[5] (a) F. Werfel, G. Drager, U. Berg, *Crys. Technol.* 1981, **16**, 119. (b) C.Z. Wu, Y. Xie, L.Y. Lei, S.Q. Hu, C.Z. OuYang *Adv. Mater.* 2006, **18**, 1727. (c) S.L.T. Anderson, *J. Chem. Soc. Faraday Trans.* 1979, **175**, 1356 (d) G.A. Sawatzki and D. Post, *Phys. Rev. B,* 1979, **20**, 1546.

[6] C.Z. Wu, P. Yin, X. Zhu, C.Z. Ouyang, Y. Xie *J. Phys. Chem. B* 2006, **110**, 17806.